Structure around the island of inversion with single-neutron knockout reactions at GANIL

B. Fernandez-Dominguez, B. Pietras, N. Patterson, J.S. Thomas, N.A. Orr, M. Chartier, W. Catford, N.L. Achouri, J.C. Angélique, N.I. Ashwood, et al.

Structure around the island of inversion with single-neutron knockout reactions at GANIL

B. Fernández-Domínguez[1,2], *B. Pietras*[1], *N. Patterson*[3], *J. S. Thomas*[3], *N. Orr*[4], *M. Chartier* [1], *W. Catford*[3], *N. L. Achouri*[4], *J-C. Angélique*[4], *N. I. Ashwood*[5], *A. Banu*[6], *B. Bastin*[4], *J. Brown*[7], *R. Borcea*[11], *S. Franchoo*[9], *M. Freer*[5], *L. Gaudefroy*[2],*B. Laurent*[4], *M. Labiche*[10], *R. C. Lemmon*[10], *F. Negoita*[11], *S. Paschalis*[1], *E. S. Paul*[1], *M. Petri*[1], *P. Roussel-Chomaz*[2], *M. Staniou*[11], *M. J. Taylor*[7], *and L. Trache*[6].

[1] Department of Physics, University of Liverpool, L69 7ZE, UK.
[2] GANIL, Bd Henri Becquerel, BP 55027, 14076 Caen-Cedex 05, France.
[3] Department of Physics, University of Surrey, Guildford GU2 5XH, UK.
[4] Laboratoire de Physique Corpusculaire, 6 bd Maréchal Juin, 14050 Caen Cedex, France.
[5] School of Physics and Astronomy, University of Birmingham, Birmingham, B15 2TT, UK.
[6] Cyclotron Institute, Texas AM University, USA.
[7] Department of Physics, University of York, Heslington, York YO10 5DD, UK.
[8] GSI, Planckstr. 1, Darmstadt 64291, Germany.
[9] Institut de Physique Nucléaire d'Orsay, 91406 Orsay, France.
[10] Daresbury Laboratory, Warrington, WA4 4AD, UK. and
[11] National Institute for Physics and Nuclear Engineering, RO-77125, Bucharest-Magurele, Romania.

Abstract

The nuclear structure of the ^{31}Mg nucleus has been studied with the single-neutron knockout reaction. We report on the preliminary results of an experiment performed with the EXOGAM array coupled, for the first time, to the SPEG spectrometer at GANIL. We present a provisional result for the inclusive single-neutron knockout cross section of σ_{inc}= 90(5) mb. Preliminary exclusive cross sections for the measured bound states, including the ground state, are also presented. Finally, preliminary longitudinal momentum distributions for the ground state and first excited state are also shown. These results are compared to Monte Carlo Shell-Model calculations in the sd-pf region.

1 Introduction

The so-called "island of inversion" region of the nuclear chart, where transitions from normal to intruder ground state configurations across the $N = 20$ shell gap occur, was first placed around $20 \leq N \leq 22$ and $10 \leq Z \leq 12$. However, for the magnesium isotopes ($Z = 12$), the prediction of the neutron boundaries for this region is still not clear. Recent experimental efforts [1-5] have provided evidence to suggest that ^{29}Mg and ^{30}Mg are outside the island of inversion, and that ^{31}Mg is within the region.

G. Neyens et al. [1] and M. Kowalska et al. [2] have determined the ground state spin, magnetic moment, and the low-lying structure of ^{31}Mg by hyperfine-structure and β – NMR measurements. Comparisons with advanced shell model calculations show that the experimental observables are correctly reproduced when allowing two neutron excitations across the $N = 20$ shell gap. The ground state wave function is, therefore, interpreted as dominated by a purely 2p-2h intruder configuration. A complementary β decay study on ^{31}Mg carried out by F. Maréchal et al. [3] finds weak feeding to the first excited states of ^{31}Al, which are of sd nature, supporting the interpretation of the previous references [1, 2].

Single-neutron knockout reactions performed at MSU by R. Terry et al. [4] have allowed a mapping of the ground state configuration of ^{30}Mg. The intruder admixture of the ground state, measured by occupation numbers of neutrons in the fp single-particle states, was found to be small with a determined value of 0.60(12) neutrons. The structure of the low-lying states of the ^{30}Mg nucleus has been studied

by means of β decay [5], Coulomb excitation [6] and β – delayed neutron decay [7]. The energies of the 0_1^+ and 2_1^+, as well as the $B(E2)$ values, are consistent with the sd shell model, confirming the $0\hbar\omega$ (or 0p-0h) structure of these states.

The study of the single-neutron knockout reaction of ^{31}Mg is a very interesting case since it is in the region where dramatic changes in single-particle structure are predicted. Indeed, ^{31}Mg is the only magnesium isotope between the normal, sd shell dominated configuration of ^{30}Mg, and the expected onset of the island of inversion at $N = 20$. The current measurement represents the "missing link" to the understanding of the neutron-deficient boundary in the Mg chain around the island of inversion. The technique of single-neutron knockout reactions is well suited to give quantitative insight into the single-particle components of the nuclear many-body wave function.

2 Experimental Set-Up

To study the structure of neutron-rich nuclei in the $sdpf$ shell region with knockout reactions, the EXOGAM array (a high efficiency Ge detector array), supplemented with NaI detectors, was coupled to the SPEG spectrometer for the first time at GANIL (France).

The primary beam of 77.5 MeV/u ^{36}S, delivered by the CSS1 and CSS2 cyclotrons with a beam power of 1 kW ($\sim 10^{13}$ particles per second) was focused on the ^{12}C SISSI target of 500 mg/cm^2 thickness, rotated by 45 degrees. The secondary beams were selected by the alpha spectrometer with an achromatic degrader at the intermediate focal plane. The central $B\rho$ of the second dipole of the alpha spectrometer was set to 2.80 Tm, while the magnetic rigidity of the first dipole was tuned to optimise the production of the light neutron-rich isotopes, namely ^{23}O and ^{25}F. However, due to the relatively large momentum acceptance of the alpha spectrometer, elements from Oxygen to Magnesium were transmitted to the SPEG spectrometer.

The secondary cocktail beam was continuously monitored with a thin scintillator and a drift chamber. A secondary ^{12}C reaction target of thickness 170 mg/cm^2 was placed at the focal point in between the SPEG analyser and the SPEG dipole. The spectrometer was operated in an achromatic mode at the target position.

Isotopic identification of the ions after the reaction target was achieved with a set of detectors near the SPEG focal plane: two drift chambers, measuring the particle trajectories (X,Y); one ionisation chamber, measuring energy loss (ΔE); and a plastic scintillator, measuring the residual energy (E). The nuclear charges of the elements were deduced from a ΔE vs E identification matrix. The isobaric identification was obtained from time-of-flight measurements between the plastic at the end of the focal plane of SPEG and the Radio Frequency from the cyclotron. Finally, to separate the projectile-like reaction products from the incoming beam particles, an additional ΔE vs focal plane position selection was applied.

The gamma rays following the de-excitation of the fragments emitted in an excited state were detected at the reaction target position with a hybrid gamma-ray detection array, consisting of 12 NaI and 8 Ge detectors. The array was arranged in a symmetric configuration: two rings of 4 highly segmented EXOGAM clovers each, were placed around 45° forward and backward at distances 215 and 134 cm, respectively. In addition, 4 clusters of 3 NaI detectors were placed at 90° at a 310 cm distance to the target. A view of the geometrical configuration is presented in Fig. 1. Total photopeak efficiency for the full EXOGAM-Ge array was 3.3% with an average energy resolution of 2.7% at 1.3 MeV.

3 Analysis and Preliminary Results

The inclusive knockout cross section of $\sigma_{inc} = 90(5)$ mb was obtained from the identified projectile-like fragments reaching the final SPEG focal plane, relative to the beam current of ^{31}Mg and the number of atoms in the target. The uncertainty in the cross section of 5% is mainly dominated by the normalisation procedure and software gates.

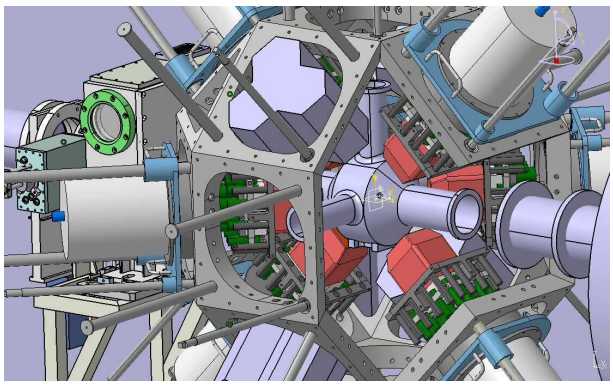

Fig. 1: Hybrid gamma detection array mounted around the target position in SPEG.

A velocity measured in an event-by-event basis in SPEG (average $\beta = 0.317$) was used to correct for the Doppler shift. The final Doppler-corrected and add-back reconstructed energy spectrum obtained from the EXOGAM array in coincidence with ^{30}Mg knockout fragments is presented in Fig. 2. A chi-squared fitting procedure was used to minimise the difference between the data and a combined simulated Geant4 response of the entire array, together with an exponential function to describe the background. From singles spectra analysis, six gamma-ray transitions have been determined in the ^{12}C(^{31}Mg,^{30}Mg+γ)X reaction. Observed transitions at energies of 988(2), 1484(1), 1822(2), 1981(2), 3534(6) keV, are consistent with the results observed in previous measurements [5–7]. A new transition at 958(2) keV, which is well resolved in the doublet near 1 MeV, has been identified in the present work. Gamma-gamma coincidences have allowed the construction of a tentative level scheme presented in Fig. 3. The new transition has given rise to a new level in ^{30}Mg at 2442(2) keV, not previously observed.

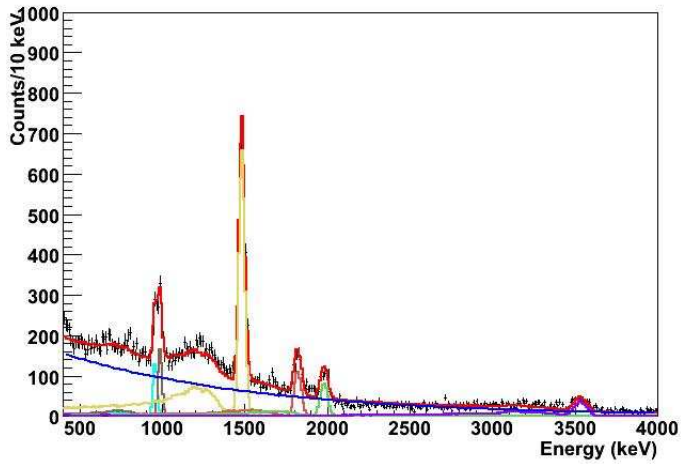

Fig. 2: Germanium γ-ray spectrum of ^{30}Mg.

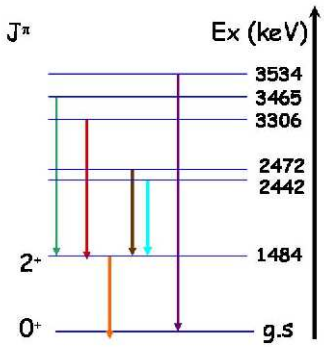

Fig. 3: Preliminary level scheme of ^{30}Mg

Exclusive cross sections to the final states in ^{30}Mg populated in the knockout reaction are summarised in Table 1. The intensity of each transition is calculated by normalising the number of detected gamma-rays, corrected by the effective efficiency, to the number of reaction products. The branch, b, for the direct population of each level was obtained by intensity balance. Only statistical uncertainties are shown. The uncertainties from the gamma-ray efficiency is expected to be lower than 4%. The ground state cross section was obtained by subtracting from the inclusive cross section all of the observed excited-state contributions.

E_{level}(keV)	E_γ(keV)	I_γ (%)	b (%)	σ(mb)
g.s.			31.3(18)	28.3(22)
1484(1)	1484(1)	53.8(10)	15.2(13)	13.7(14)
2442(2)	958(2)	6.1(3)	6.1(3)	5.5(4)
2472(2)	988(2)	7.9(3)	7.9(3)	7.2(5)
3306(2)	1822(2)	13.3(5)	13.3(5)	12.0(8)
3465(2)	1981(2)	11.1(3)	11.1(3)	10.0(7)
3534(6)	3534(6)	14.9(8)	14.9(8)	13.4(10)

Table 1: Results for the ^{12}C(^{31}Mg,^{30}Mg)X reaction. The proposed energy levels, and transition energies as well as the transition intensities I_γ, direct population branches b, and the resulting cross sections σ are given.

The longitudinal momentum distributions of the knockout fragment ^{30}Mg were measured in the SPEG spectrometer. The eikonal calculations describing the reaction mechanism have been folded with the experimental filter including the beam spread, energy loss and angular straggling, and the resolution of the spectrometer. This observable characterises the relative orbital angular momentum of the neutron removed from the projectile ground state wave function. The preliminary experimental results for removal to the ground state and first excited state of ^{30}Mg are compared to the theoretical calculations in Fig. 4 and Fig. 5, respectively. Due to the large acceptance of the SPEG spectrometer, acceptance corrections are less than 2-3%. The ground state distribution is in good agreement with $\ell = 0$, confirming the spin and parity assignment of $1/2^+$ for ^{31}Mg found by G. Neyens et al. [1]. The first excited state presents a much broader distribution, suggesting an assignment of $\ell = 2$, consistent with the assignment reported in [5].

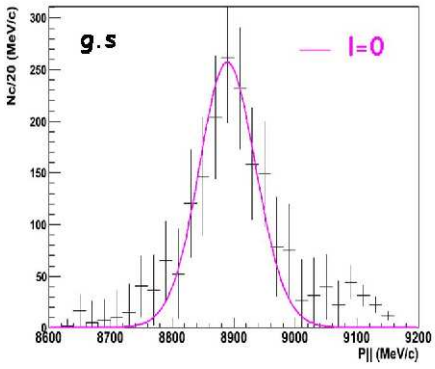

Fig. 4: Longitudinal momentum distribution for the ground state in ^{30}Mg

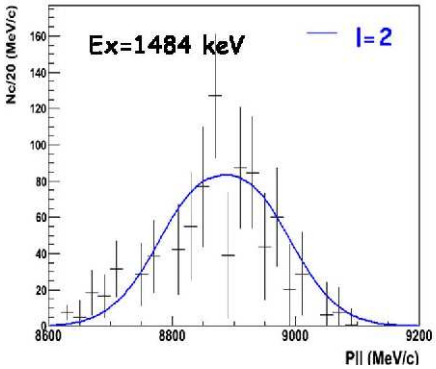

Fig. 5: Longitudinal momentum distribution for the first excited state in ^{30}Mg

4 Discussion

In Table 2 exclusive cross sections are compared to the single-particle cross sections , σ_{sp}, calculated using the reaction theory described in references [8, 9]. Deduced spectroscopic factors are compared to Monte Carlo shell model calculations using the SDPF-M interaction [10] provided by Y. Utsuno et al [11].

The results obtained from the SDPF-M calculations show a significant disagreement with the experimental values. The measured spectroscopic factor for the ground state is around 5 times larger than the shell model predictions. On the other hand, the first-excited state shows a 33% lower value than

Table 2: Theoretical and experimental spectroscopic factors

E_c^{th}(MeV)	J^π	nlj	C^2S_{th}	E_c^{exp}(MeV)	l	σ_{sp}(mb)	C^2S_{exp}
g.s.	0^+	$2s_{1/2}$	0.10	g.s.	0	28.3	0.51(4)
1.56	2^+	$1d_{3/2}$	0.92	1.48	2	13.7	0.62(6)

the predicted one. Although not all the experimental uncertainties have been applied, in total they are expected to be lower than 10%–still not significant enough to account for the differences between theory and results. There is still no clear explanation for the disagreement. For the ground state exclusive cross section (hence, deduced spectroscopic factor) to be in closer agreement with the theoretical prediction, a significant fraction of gamma transition strength would have to have gone unobserved. These presumably higher-lying, unobserved transitions would lead to a reduction in the proportion of the inclusive cross section attributed to the direct population of the ground state of ^{30}Mg. This seems unlikely.

5 Conclusions

Preliminary results on single-neutron knockout measurements from ^{31}Mg have been discussed. Longitudinal momentum distributions for the ground state and first excited state show a good agreement with $\ell = 0$ and $\ell = 2$ values, respectively. Preliminary spectroscopic factors are compared to SDPF-M calculations. The significant discrepancies between the theory predictions and the experimental results could lead to some revision of the picture of ^{31}Mg.

References

[1] G. Neyens et al., Phys. Rev. Lett. **94**, 022501 (2005)
[2] M. Kowalska et al., Phys. Rev. C **77**, 034307 (2008)
[3] F. Marechal et al., Phys. Rev. C **72**, 044314 (2005)
[4] J. R. Terry et al., Phys. Rev. C **77**, 014316 (2008)
[5] P. Baumman et al., Phys. Rev. C **39**, 626, (1989)
[6] O. Niedermaier et al., Phys. Rev. Lett. **94**, 172501 (2005)
[7] H. Mach et al., Eur. Phys. J. A **25**, s01 105-109, (2005)
[8] J. A. Tostevin et al., Nucl. Phys. A **682**, 320c, (2001)
[9] J. A. Tostevin et al., J. Phys. G **25**, 735, (1999)
[10] Y. Utsuno et al., Phys. Rev. C **50**, 054315 (1999).
[11] Y. Utsuno et al., Private Communication (2009).